CTRL: A Self-Organizing Femtocell Management Architecture for Co-Channel Deployment

Ji-Hoon Yun and Kang G. Shin

Real-Time Computing Laboratory, EECS Department
The University of Michigan, Ann Arbor, MI 48109-2121, U.S.A.
{jihoony, kgshin}@eecs.umich.edu

ABSTRACT

Femtocell technology has been drawing considerable attention as a cost-effective means of improving cellular coverage and capacity. However, under co-channel deployment, femtocells may incur high uplink interference to existing macrocells, and vice versa. To alleviate this interference, we propose a distributed and self-organizing femtocell management architecture, called CTRL (**C***omplementary* **TR***i-control* **L***oops*), that consists of three control loops. First, for protection of macrocell users' uplink communications, CTRL controls the maximum TX power of femtocell users based on the feedback macrocell's load margin so as to keep, on average, the macrocell load below a certain threshold. Second, CTRL determines the target SINRs of femtocell users, conditioned on the maximum TX power, to reach a Nash equilibrium based on their utility functions, thus achieving efficient coordination of uplink usage among femtocells. Third, for protection of femtocell users' uplink communications, the instantaneous TX power of each femtocell user is controlled to achieve the target SINR against bursty interference from nearby macrocell or femtocell users.

Our in-depth evaluation has shown CTRL to successfully preserve the macrocell users' service quality from femtocells' interference and converge to an optimal point under highly dynamic user TX conditions. CTRL is also shown to limit the effects of the estimation errors of channel gains and feedback delay.

Categories and Subject Descriptors

C.2.1 [**Computer-Communication Networks**]: Network Architecture and Design—*Wireless communication*

General Terms

Algorithms, Design, Performance, Theory

Keywords

Femtocell, home base station, co-channel deployment, interference mitigation, self-organizing networks

MobiCom'10, September 20–24, 2010, Chicago, Illinois, USA.

1. INTRODUCTION

Femtocell technology has emerged as a cost-effective means to enhance indoor network coverage and capacity for growing demands for cellular (voice calls and data) services within a home or an enterprise environment [1]. A *femtocell* is a small indoor area covered by a low-power base station (BS), referred to as a *femto BS* in this paper. Unlike macro BSs, femto BSs are installed on the subscriber's premise and typically connected to an operator's core network via public Internet connections, such as DSL and cable modems. Femtocells benefit both subscribers and operators; better voice coverage and higher indoor data throughput for subscribers, and macrocell offloading and indoor coverage improvement at low capital and operational costs for operators.

A main challenge associated with the femtocell technology is how to protect, under co-channel deployment, macrocell user services against interference from femtocells while exploiting as high spatial reuse of channel resources as possible within femtocells. Due to the high cost of a licensed spectrum, operators may allocate femtocells the same carrier frequency as macrocells, called *co-channel deployment*. Under co-channel deployment, transmissions within femtocells may cause interference to user services within macrocells, and vice versa [2]. Such a phenomenon has been reported as a serious problem in uplink (UL) communications [3–6]. The resultant performance degradation makes the femtocell technology's market penetration difficult since the deteriorated service to existing users will increase the churn rate. It is, therefore, important to solve this interference problem by managing femtocells efficiently and effectively.

The distinct features of femtocell technology impose the following requirements on femtocell management. First, considering the fact that femtocells are to be deployed on an already-existing and working cellular infrastructure, the femtocell management should minimize the change of a performance-critical part of macro BSs, especially radio resource management (RRM). The RRM within existing macrocells has been optimized and validated in the field under a wide range of cell conditions, e.g., traffic patterns, quality-of-service (QoS), and user mobility. Changing the macrocell RRM may require tedious and time-consuming optimizations. Second, salient features of femtocells, such as user installation and unplanned deployment, require femtocell management to be *distributed* and *self-organizing*, and hence, convergence becomes a critical factor. These features, along with its restricted access, make the femtocell management very different from the classical hierarchical cell coordination problem. Besides, supporting legacy user devices without using any special hardware is another important requirement.

There have been a few proposals to resolve the femtocell interference problem in UL communications, but they have, unfortunately, several limitations. Vikram *et al.* [4] proposed a coordinated UL

power-control architecture for both macro- and femto-cells, which requires macrocells to use their proposed power-control algorithm. Jo *et al.* [6] proposed a simple up/down UL power control for femtocells. Their scheme adjusts the transmit (TX) power of femtocell users in proportion to the fed-back interference level of macrocells and does not require any change of the macrocell RRM. However, they focused only on the protection of a macrocell's UL communication and their scheme does not guarantee convergence either. Moreover, both proposals did not consider the feedback delay. Yavuz *et al.* [3] proposed an attenuator adjustment scheme restricted to femtocell UL protection against nearby macrocell users. Proposals for protection of downlink (DL) communications [5, 7] are neither effective nor optimal for UL communications as they operate based only on a femtocell's local condition, ignoring the macrocell's UL state. Sundaresan and Rangarajan's recent study [8] focused on OFDMA-based femtocell systems, mainly dealing with orthogonal assignment of time-frequency resources between macro- and femto-cells: *strictly orthogonal* in the isolated model and *orthogonal* between neighboring macrocell and femtocell users only in the coupled model for higher total utility. However, both of these models require modification of the macrocell RRM due to their tightly-coupled coordination of macro- an femto-cells without considering the other requirements.

To overcome the above limitations of existing schemes in single-carrier cellular systems, we propose a distributed and self-organizing femtocell management architecture for UL communications, called **C***omplementary* **TR***i-control* **L***oops* (CTRL). The key idea behind CTRL is the use of multiple control loops optimally designed with different objectives while complementing each other toward a common goal. These control loops and their complementary interactions are summarized as follows.

- *Maximum transmit power control* (MTXPC) loop protects the macrocell's UL communication against the interference from femtocells. This is achieved by controlling the maximum TX power of femtocell users based on the macrocell UL load margin fed back with delay such that the macrocell load does not exceed, on average, a given threshold.
- *Target signal-to-interference and noise ratio control* (TSINRC) loop enables utility-optimal resource coordination among femtocells without signaling between them while being conditioned on the maximum TX power constraint obtained by the MTXPC loop. The control algorithm is designed to achieve a Nash Equilibrium for general utility functions.
- *Instantaneous transmit power control* (ITXPC) loop protects the femtocell's UL communication against bursty interference from nearby macrocell or femtocell users. It controls the TX power of a femtocell user such that the target SINR determined by the TSINRC loop is achieved on a small timescale (e.g., frame).

CTRL meets all the requirements mentioned earlier. That is, CTRL does not require modification of the RRM of macro BSs, thus enabling smooth migration of co-channel femtocells into existing cellular networks. The control algorithms of CTRL also achieve convergence under the provided conditions against time-varying and unpredictable environmental changes, such as interference, threshold value, etc. Besides, CTRL is compatible with legacy user devices since it does not impose any non-standard operation on them. CTRL is software-based, does not increase the hardware cost, and can be improved further with an extra receiver module enabling the over-the-air feedback (as detailed in Section 3).

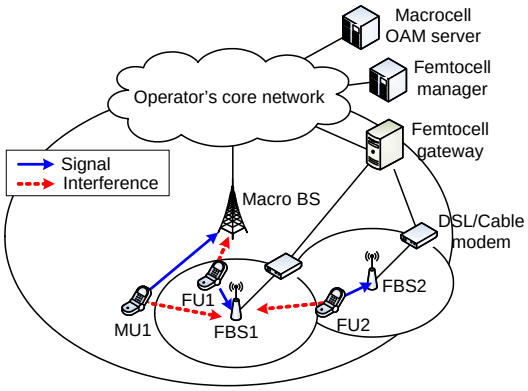

Figure 1: Uplink interference scenarios under co-channel femtocell deployment

Our evaluation results show that CTRL successfully protects a macrocell's uplink service regardless of the number of femtocells in the macrocell. In an example scenario with 50 macrocell users and 100 femtocell users per macrocell, 96% of macrocell users meet the specified service quality while only 8% of them meet it without CTRL. Moreover, CTRL converges to an optimal point under a wide range of user traffic dynamics and maintains stability against up to 100% errors in estimating the channel gains and feedback delay.

The rest of this paper is organized as follows. Sections 2 and 3 describe the motivation of this work and the system model, respectively. Section 4 presents the CTRL architecture, and Section 5 describes the control algorithms. Section 6 evaluates the CTRL architecture using simulation, and Section 7 concludes the paper.

2. MOTIVATION

We first advocate the necessity of femtocell management for UL communications. Then, we discuss the requirements of femtocell management and identify the limitations in applying existing techniques to femtocell networks.

2.1 Why Femtocell Management for UL Communications?

The initial motivation behind the introduction of femtocells to cellular networks was extension of indoor coverage for voice calls. However, the femtocell technology provides an important additional advantage, especially for data services: overall data capacity improvement due to spatial channel reuse and macrocell offloading. Subscribers also have incentives to use femtocells even within a macrocell coverage for better indoor data throughput, less device power consumption (longer battery life) and possibly an unlimited data plan. Under the expected co-channel femtocell deployment, however, UL transmissions of femtocell users (users being served by femtocells) may cause interference to the ongoing UL transmissions of users being served by macrocells, and vice versa. Several researchers [3–6] reported such a phenomenon and the resultant performance degradation of both macrocell and femtocell users in UL communications as a serious problem.

We illustrate possible UL interference scenarios between macro- and femto-cells in Fig. 1 as follows. Due to their unplanned deployment, some femtocells (FBS1) could reside close to a macro BS and their users (FU1) will incur high UL interference to the macro BS. The opposite may also happen when a macrocell user(s) (MU1) resides in the vicinity of a femto BS (FBS1). To make mat-

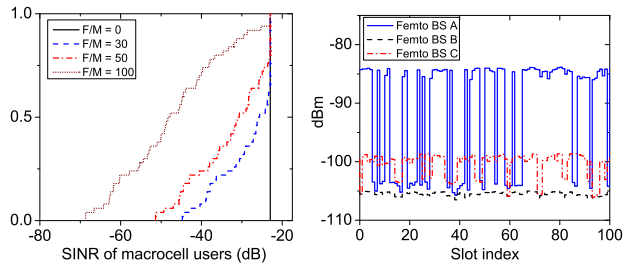

Figure 2: Illustration of the femtocell UL interference problem: cumulative distribution of macrocell users under a varying number of femtocells (left) and UL interference evolution samples at three different femto BSs (right)

ters worse, the users of the femto BS in such a situation get to use stronger TX power to maintain good receiving SINR, incurring higher UL interference to the macrocells around them. A macrocell user induces higher interference to nearby femto BSs as it is farther away from its serving macrocell. Another possible interference source to a femtocell's UL (FBS1) is neighboring femtocells (FBS2). Unplanned deployment could make multiple femtocells reside in a neighborhood, possibly resulting in severe performance degradation without proper coordination between them. On the other hand, unlike the UL interference to a macro BS, that to a femto BS (FBS1) may result from a small number of wireless sources (MU1 and FU2), and thus, the pattern could be bursty. The usual power control schemes are not designed to deal with this bursty interference [3].

The femtocell UL interference was also observed in our two-tier multi-cell simulations under a realistic environmental configuration (as detailed in Section 6.2). The left figure in Fig. 2 demonstrates the macrocell users' UL performance degradation due to randomly-deployed femtocells. In the absence of femtocell users, all macrocell users meet the target SINR (-20.96 dB). As the number of femtocells within a macrocell (denoted by F/M in the figure) increases, the macrocell users' achieved SINRs get deteriorated significantly. At the same time, the level of inter-femtocell interference also increases; the average UL interference of femto BSs was -80.0, -76.5 and -74.1 dBm for F/M = 30, 50 and 100, respectively. The UL interference at each femto BS was bursty as illustrated in the right figure of Fig. 2. The degree of burstiness differs for different femto BSs, depending on the presence of nearby macrocell or femtocell users.

Therefore, without well-designed femtocell management, both macrocell and femtocell users will experience performance deterioration. Based on the above observations, we can summarize the objectives of femtocell management: (1) protection of macrocell's UL communication against femtocell interference; (2) efficient resource coordination among femtocells; and (3) protection of femtocell's UL communication against bursty interference. In general, femtocells play a supplementary role in cellular networks. Hence, we assume that the first objective is given the highest priority.

2.2 Requirements of Femtocell Management

Due to the overlaid deployment on existing cellular networks[1] and other salient features of femtocells, the following requirements need to be imposed when designing a femtocell management architecture.

- *No change of macrocell RRM:* The RRM within existing macrocells has been optimized and verified in the field to provide various types of service under a wide range of cell conditions, such as traffic patterns, user population, QoS, user mobility, etc. So, changing the macrocell RRM may influence already-stabilized macrocell user services and accompany costly optimizations.
- *Distributed and self-organizing operation:* Due to end-users' installation and unplanned deployment of a possibly large number of femtocells, femtocell management should be distributed and self-organizing. Thus, convergence under time-varying and unpredictable environmental changes is an essential requirement.
- *Support of legacy user devices:* Supporting existing user devices is an important requirement for market penetration. To meet this requirement, a management architecture should not impose any new operation on user devices.
- *No special hardware:* For cost-efficiency, a femto BS should not be required to be equipped with special hardware.

2.3 Limitations of Existing Techniques

There have been several proposals for resolving the femtocell DL interference problem, mainly focusing on avoidance of excessive DL interference to macrocell users in the vicinity of a femto BS. Power adaptation is to let a femto BS use as low DL TX power as possible while serving its users. It is shown in [7] that such a technique is good at mitigating femtocell DL interference to macrocell users. Femtocell sectorization [5] radiates RF energies only within sectors with users and thus reduces the possibility of getting nearby macrocell users interfered with. It requires a sectorized antenna and multiple radio paths, one for each sector. Likewise, beamforming will be also effective, but at the expense of increased hardware cost. The above-mentioned schemes operate based on the femto BS's local information only and regardless of the macrocell UL status. Therefore, they are not effective against the UL interference. Although femtocell sectorization may reduce the required UL TX power of femtocell users thanks to directional interference reception at the serving femto BS, UL interference from femtocells to macrocells is still uncontrollable and protection of the macrocell's UL communication is not guaranteed, either.

There have been a few proposals for tackling the UL interference, but they do not satisfy all the requirements or objectives discussed earlier. Vikram *et al.* [4] proposed a non-cooperative game-theoretic UL power-control architecture for both macro- and femtocells, based on Ji and Huang's study [9]. They consider macrocell users as game players and thus restrict the RRM of macrocells to the utility function and actions specified by the game. The scheme proposed by Jo *et al.* [6] adjusts the TX power of femtocell users in proportion to the fed-back interference level of macrocells and does not require any change of the macrocell RRM. However, they focused on protecting a macrocell's UL only without providing any convergence analysis. In addition, none of these two schemes considered the feedback delay that influences the convergence of an algorithm. Yavuz *et al.* [3] proposed an attenuator adjustment scheme in which a femtocell user under high UL interference is given room for increasing its TX power thanks to the increased attenuation. This scheme is restricted to femtocell UL protection.

There was a recent proposal targeting OFDMA systems by Sundaresan and Rangarajan [8]. In their isolated model, a macro BS

[1] In general, macrocells are deployed first since nationwide connectivity is crucial for cellular services.

and femto BSs are allocated orthogonal time-frequency resources while the coupled model imposes this constraint on neighboring macrocell and femtocell users to achieve higher total utility. To realize these two models, each femto BS requires time synchronization with a macro BS and an extra receiving module with self-interference cancellation capability for overhearing macrocell signals (neither of them is required in CTRL; difficulties and some solutions of the over-the-air feedback will be discussed in Section 3.2). Moreover, both models require modification of macro BSs' RRM for dynamic adjustment of resource split.

3. SYSTEM MODEL

This section describes the network architecture under consideration and two implementation alternatives for macrocell-load feedback.

3.1 Network Architecture

We consider a single-carrier cellular system (e.g., CDMA) and a typical two-tier femtocell network architecture depicted in Fig. 1 where femtocells are overlaid on macrocells. The set of macrocells $\mathcal{M} = \{1, \ldots, M\}$ and the set of femtocells $\mathcal{F} = \{1, \ldots, F\}$ use an identical carrier frequency. Cell m operates under BS m. The set of macrocell users and that of femtocell users are represented by $\mathcal{M}_u = \{1, \ldots, M_u\}$ and $\mathcal{F}_u = \{1, \ldots, F_u\}$, respectively. The channel gain from user i to BS j is denoted by $h_{i,j}$. We assume that user i transmits data with the activity factor a_i ($0 \leq a_i \leq 1$).

As in general cellular networks, every BS has a logical connection to an Operation, Administration and Management (OAM) server that BSs receive initial configuration settings from and occasionally report their status to. We refer to the OAM server dedicated to femtocells as the *femtocell manager*.

3.2 Macrocell-Load Feedback

For protection of macrocell users' UL communications, femto BSs need to know the current status of macrocells—as was assumed in [4, 6]—which can be enabled by the feedback from macro BSs, referred to as *macrocell feedback*. We assume that a macro BS feeds back its *cell load margin* defined as the difference between the current cell load and a given load threshold; the cell load margin is positive when the current load is lower than the threshold, else it is negative. Two implementation alternatives for macrocell feedback, differing in delay and cost, are described next.

3.2.1 Feedback over wired networks

First, we consider the approach that femto BSs receive macrocell feedback through the operator's wired network. To realize this, each macro BS periodically reports its cell load margin to the OAM server. Then, the macrocell OAM server forwards it to the femtocell manager. Finally, the femtocell manager sends it to the femto BSs that have subscribed to the feedback of the macro BS. Note that signaling interfaces for OAM are generally vendor-specific. To receive the feedback from proper macro BSs, femto BSs need to execute a subscription procedure; when powered on, a femto BS scans neighbor macrocells and reports the list of macrocell feedback subscriptions to the femtocell manager.

'Feedback over wired networks' does not require additional hardware of femto BSs, but has a larger delay than the other approach.

3.2.2 Feedback over the air

In the second approach, femto BSs receive macrocell feedback directly from macro BSs over the air. Specifically, macro BSs broadcast their load margin information which is then overheard by femto BSs. This approach requires two issues to be resolved:

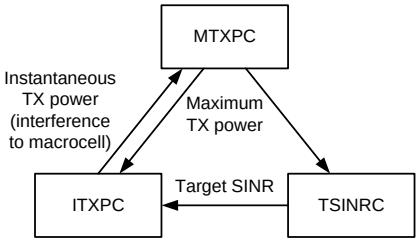

Figure 3: Complementary interactions between control loops

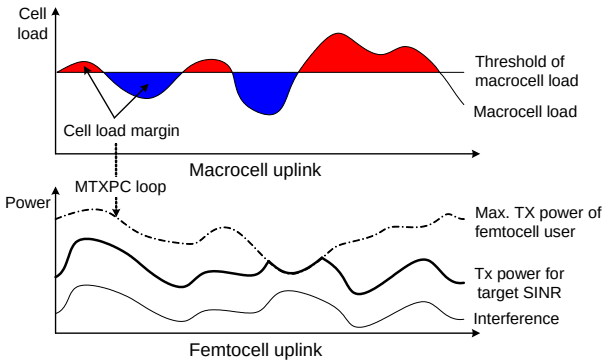

Figure 4: Overview of the CTRL concept

implementation feasibility and standard violation. We discuss each of them next.

In the case of frequency-division duplex (FDD), femto BSs need to overhear macrocell signals at a frequency other than their original RX frequency, i.e., they require an extra receiver module. The time-division duplex (TDD) also requires this to enable full duplexing (receiving macrocell signals during an active transmission). On the other hand, if macro BSs feed back information using the same frequency that femto BSs use to transmit data, femto BSs may not be able to demodulate macrocell signals due to significant self-interference. This problem can be addressed by (1) the macrocell's feedback at a frequency different from the femtocell's TX frequency or (2) interference cancellation as in wireless relays [10]. The first solution is applicable only when macro BSs use multiple carrier frequencies[2] while the latter increases the cost.

In order to broadcast the load-margin information, modification of the legacy system information (SI) format [11] is required. In general, operators do not use every SI field in the standards. Thus, some unused SI fields can be exploited for the inclusion of feedback.

The delay of feedback over the air is the air propagation delay from a macro BS to femto BSs which is negligibly small.

4. THE CTRL ARCHITECTURE

We first present the architecture of CTRL and its basic concept and design rationale. Then, we formulate the problems for the design of control algorithms for the CTRL architecture.

4.1 Overview of CTRL

The goal of CTRL is to achieve all the objectives listed in Section 2.1 (with the highest priority on protection of macrocell UL communications) while meeting the requirements discussed in Sec-

[2]This is the typical case in urban areas due to high traffic demands.

tion 2.2. Each of the objectives can be considered as a subproblem of the femtocell interference problem. CTRL solves these subproblems individually using different control loops, constrains one loop's result by the others' according to the relationship depicted in Fig. 3, and finally produces a coordinated result. All decisions of the three control loops for a user are made by the femto BS that the user is connected to, based on the specified interaction rule between them. In what follows, we describe each of these control loops and their complementary interactions.

4.1.1 MTXPC Loop

The MTXPC loop is responsible for protecting a macrocell's UL communication by controlling the maximum TX power of femtocell users based on the fedback macrocell load margin. A positive macrocell load margin indicates that the macrocell has room for accommodating additional load, while a negative margin means that the macrocell is overloaded (Fig. 4). Assuming that a cell's UL load is a monotonically increasing function of the total received power,[3] controlling the TX power of femtocell users to keep the average macrocell's UL load below a given threshold. Macrocell users' UL performance, therefore, will not be degraded below a specific level. An important feature of the MTXPC loop is that it controls the femtocell users' maximum TX power, *not* their instantaneous TX power. Such an approach allows the other control loops to perform further optimizations of femtocells based on their local condition.

The UL load of a macrocell comes from three components: intra-macrocell user traffic, other macrocells' interference, and femtocell interference. By giving priority to the macrocell users, the maximum load that femtocell users are allowed to contribute is computed by subtracting the intra-macrocell and other macrocells' loads from the load threshold. However, a macro BS cannot distinguish other macrocells' interference from the femtocells' interference, and moreover, other macrocells' interference is not controllable. So, it cannot allocate an exact load portion to femtocells. Instead, a macro BS simply provides its current load margin which will vary with time. Then, based on the margin, femtocells should adapt their resource usage to their unknown share. We tackle this difficulty by modeling the unpredictable other macrocells' interference as a disturbance from a control-theoretic perspective.

4.1.2 TSINRC Loop

The TSINRC loop enables efficient coordination of resource usage among neighboring femtocells based on local information, such as user-specific UL interference, activity, channel condition, etc. The coordination is achieved without signaling between femto BSs since no inter-femto BS signaling interface has been defined in standards.[4] Therefore, femto BSs need to infer the current condition based on implicit feedback, such as interference level and achieved SINR. Finally, the result is conditioned on the maximum TX power constraint obtained via the MTXPC loop.

4.1.3 ITXPC Loop

Although the TSINRC loop determines the target SINR, the short-term achievable SINR may fluctuate due to bursty interference (as mentioned in Section 2.1), resulting in inconsistent user service quality. The source of interference is nearby macrocell users or femtocell users being served by other femtocells. The ITXPC loop controls the instantaneous TX power of a femtocell user on a small time-scale (e.g., frame) such that the target SINR determined by the TSINRC loop is achieved on a short-term scale, as shown in Fig. 4. If we simply set the TX power to the target SINR multiplied by the current interference, an abrupt change of interference due to the TX ON/OFF of a nearby user will lead to a drastic change of the TX power and the interference to both macrocell and femtocell users. This type of sudden interference has a detrimental effect on performance even when the average interference level is low. Thus, the ITXPC algorithm should be designed to converge with neither overshoot nor oscillation. Finally, the TX power levels of femtocell users determined by the corresponding ITXPC loops collectively form the femtocell interference to a macro BS, and hence influence the MTXPC loop. The result of the ITXPC loop is also conditioned on the maximum TX power constraint obtained via the MTXPC loop.

4.2 Problem Formulation

Throughout the paper, a user's TX power is defined as the power he uses to transmit data. Then, the amount of the radiated power per unit of time is obtained by multiplying his activity factor to the user's TX power. Let p_i and P_i denote the femtocell user i's TX power and maximum TX power, respectively. We also use γ_i to denote the femtocell user i's achieved SINR. For $\mathcal{F}_u$, we define the following three vectors:

- TX power vector $\mathbf{p} \triangleq [p_1, p_2, \cdots, p_{F_u}]^T$;
- Maximum TX power vector $\mathbf{P} \triangleq [P_1, P_2, \cdots, P_{F_u}]^T$;
- SINR vector $\boldsymbol{\gamma} \triangleq [\gamma_1, \gamma_2, \cdots, \gamma_{F_u}]^T$.

Then, the algorithms of the control loops aim to find the above three vectors that meet their objectives. Let $\mathbf{p}^*$, $\mathbf{P}^*$ and $\boldsymbol{\gamma}^*$[5] be the solution vectors.

The problems of the control loops are denoted by $P1$ (MTXPC), $P2$ (TSINRC), and $P3$ (ITXPC). Let $L^m_{th}(t)$ and $L^m(t)$ be the load threshold and the load of macrocell m at time t, respectively. We define $e_m \triangleq L^m_{th} - L^m$ as the *load margin* of macrocell m. Then, the objective of $P1$ is to make both $[e_m(t)]^+$ and $[e_m(t)]^-$ converge to 0[6] for protection of the macrocell's UL service and maximization of spatial reuse within femtocells, respectively. Thus, $P1$ is formulated as

$$P1: \quad \min_{\mathbf{P}} \lim_{t\to\infty} |e_m(t)| \text{ for } m \in \mathcal{M}. \tag{1}$$

L^m is composed of macrocell user portion L^m_M and femtocell user portion L^m_F such that $L^m(t) = L^m_M(t) + L^m_F(t)$ and $L^m_F(t) = \Gamma_m(I^m_F(\mathbf{p}))$ where $I^m_F(\mathbf{p}) = \sum_i a_i h_{i,m} p_i$ and $\Gamma_m : \mathbb{R} \to \mathbb{R}$ is an interference-to-load function which is monotonically increasing in I^m_F. As mentioned earlier, the MTXPC loop controls $\mathbf{P}$ although L^m_F is a function of $\mathbf{p}$. The only relationship between them is $\mathbf{p} \preceq \mathbf{P}$.[7] We show below the validity of this upper-bounding approach, i.e., the existence of $P1$'s solution.

PROPOSITION 1. *If there exists feasible* $\mathbf{p}^*$ *such that* $e_m = 0$, *so does* $\mathbf{P}^*$.

PROOF. Since $I^m_F(\mathbf{p}) \le I^m_F(\mathbf{P})$ and Γ is a monotonically increasing function, $\Gamma_m(I^m_F(\mathbf{p})) \le \Gamma_m(I^m_F(\mathbf{P}))$. Suppose $0 \le \Gamma_m < \infty$. Then, there always exists $\varepsilon \ge 0$ such that $\Gamma_m(I^m_F(\mathbf{P})) = \Gamma_m(I^m_F(\mathbf{p}^*)) + \varepsilon$. $I^m_F(\mathbf{P}) = \Gamma^{-1}_m(\Gamma_m(I^m_F(\mathbf{p}^*)) + \varepsilon)$ and, due to the monotonicity of Γ_m, there also exists $\varepsilon' \ge 0$ such that $I^m_F(\mathbf{P}) = \Gamma^{-1}_m(\Gamma_m(I^m_F(\mathbf{p}^*))) + \varepsilon' = I^m_F(\mathbf{p}^*) + \varepsilon'$. Here, $I^m_F(\mathbf{P}) =$

[3] This is generally acceptable in CDMA-based cellular networks.

[4] In 3GPP Long-Term Evolution (LTE) networks, the inter-BS interface, called X2, is defined only between macro BSs.

[5] $\boldsymbol{\gamma}^*$ means the target SINR vector

[6] $x^+ = \max\{x, 0\}$ and $x^- = \min\{x, 0\}$

[7] The curled inequality symbol $\succeq$ (and its strict form $\succ$) represents component-wise inequality.

$I_F^m(\mathbf{p}^*) + \varepsilon' \geq 0$, and thus, it forms an affine hyperplane in an F_u-dimensional Euclidean space of $\mathbf{P}$ lower-bounded by $\mathbf{p}^*$, which ensures the existence of $\mathbf{P}^*$ (ε is determined by the other two control loops). □

We formulate $P2$ as a non-cooperative N-player game in which each femtocell maximizes its utility function without signaling to the others, while being conditioned on the solution of $P1$, i.e., $\mathbf{P}^*$:

$$P2: \max_{p_i \leq P_i^*, \gamma_i} u_i(p_i, \gamma_i) \text{ for } i \in \mathcal{F}_u \tag{2}$$

where u_i is the utility function of femtocell user i. Finally, $P3$ is to make $e_i \triangleq \gamma_i^* - \gamma_i$ converge to 0 for $i \in \mathcal{F}_u$ where γ_i^* is the solution of $P2$. Thus, $P3$ is expressed, similarly to $P1$, as

$$P3: \min_{p_i \leq P_i^*} \lim_{t \to \infty} |e_i(t)| \text{ for } i \in \mathcal{F}_u. \tag{3}$$

5. CONTROL ALGORITHMS

We now present control algorithms to solve the problems $P1$–$P3$.

5.1 MTXPC Algorithm

$P1$ can be considered as a steady-state tracking problem from a control-theoretic point of view, i.e., a control effort is made to let a macrocell's load track the specified threshold value. Here, e_m is interpreted as the tracking error.

To detail the algorithm, we consider the *rise over thermal* (RoT) as a cell load metric, i.e., $L^m = (I^m + \sigma^2)/\sigma^2$, where I^m is the total power received at macro BS m and σ^2 the thermal noise. RoT has been widely used to represent a cell load, especially in CDMA-based cellular networks [12]. Then, $e_m = (I_{th}^m - I^m)/\sigma^2$. Without loss of generality, we can simply let $e_m = I_{th}^m - I^m$. Let I_M^m and I_F^m denote the signal strengths received at macro BS m from macrocell users and femtocell users, respectively, so that $I^m = I_M^m + I_F^m$. For simplicity of presentation, we drop the superscript m.

Let T be the macrocell feedback interval, then the MTXPC loop can be modeled as a discrete-time system whose state changes at interval boundaries. Let $v(k)$ denote variable v during the k-th interval, i.e., $[kT, (k+1)T)$. Then, $e(k)$ is written as

$$e(k) = I_{th}(k) - I(k) = I_{th}(k) - I_M(k) - I_F(k). \tag{4}$$

The MTXPC loop can be represented as a closed-loop control system depicted in Fig. 5(a). The chain reaction shown in the figure can be explained as follows. A macro BS sends e to the femto BSs subscribing to its feedback. Suppose that the femto BSs receive e with the feedback delay d (represented as z^{-d} in the figure). Upon reception of e, the femto BSs update P_i of their users with the user-specific controller D_i. Then, p_i is determined by the other two control loops and upper-bounded by P_i. We can thus let $p_i(k) = P_i(k) - \varepsilon_i(k)$ where $0 \leq \varepsilon_i(k) \leq P_i(k)$. $\varepsilon_i(k)$ varies with time according to user i's local condition. Finally, I_F is updated as

$$\begin{aligned} I_F(k) &= \textstyle\sum_{i \in \mathcal{F}_u} a_i h_i p_i(k) \\ &= \textstyle\sum_{i \in \mathcal{F}_u} a_i h_i (P_i(k) - \varepsilon_i(k)) \\ &= \textstyle\sum_{i \in \mathcal{F}_u} a_i h_i D_i(e(k-d)) - \varepsilon(k) \end{aligned} \tag{5}$$

where $\varepsilon \triangleq \sum_{i \in \mathcal{F}_u} a_i h_i \varepsilon_i$. Applying the z-transform to Eqs. (4) and (5), and combining the results, we get[8]

$$\begin{aligned} I_F(z) = \; & \frac{z^{-d} \sum_{i \in \mathcal{F}_u} a_i h_i D_i(z)}{1 + z^{-d} \sum_{i \in \mathcal{F}_u} a_i h_i D_i(z)} (I_{th}(z) - I_M(z)) \\ & + \frac{1}{1 + z^{-d} \sum_{i \in \mathcal{F}_u} a_i h_i D_i(z)} \varepsilon(z). \end{aligned} \tag{6}$$

5.1.1 Decoupling of Feedback Delay Component

The control system of Fig. 5(a) is difficult to analyze since it contains the delay component z^{-d} within the feedback loop [13]. Thus, we consider an equivalent system in Fig. 5(b) where the delay component is moved out of the feedback loop and the user-specific controller is redefined as D_i^*. Here, for ease of design, we temporarily ignore ε. Later, we prove in Proposition 3 that the resultant system works as desired even with non-zero ε. Using a similar procedure to Eq. (6), I_F of the equivalent system, denoted by I_F^{eq} for distinction, is obtained as

$$I_F^{eq}(z) = \frac{\sum_{i \in \mathcal{F}_u} a_i h_i D_i^*(z)}{1 + \sum_{i \in \mathcal{F}_u} a_i h_i D_i^*(z)} z^{-d} (I_{th}(z) - I_M(z)) \tag{7}$$

and, by equating $I_F(z)$ and $I_F^{eq}(z)$, we have

$$\sum_{i \in \mathcal{F}_u} a_i h_i D_i(z) = \frac{\sum_{i \in \mathcal{F}_u} a_i h_i D_i^*(z)}{1 + (1 - z^{-d}) \sum_{i \in \mathcal{F}_u} a_i h_i D_i^*(z)}. \tag{8}$$

Then, we can define $D_i(z)$ as

$$D_i(z) = \frac{D_i^*(z)}{1 + (1 - z^{-d}) \sum_{i \in \mathcal{F}_u} a_i h_i D_i^*(z)} \tag{9}$$

which satisfies Eq. (8). That is, if we use this D_i, the system becomes equivalent to that of Fig. 5(b). This type of controller is called *Smith predictor* [13] which is known to offer better response than classical (PID or PI) controllers if there exists a time lag within a control loop [14]. Conceptually, the Smith predictor feeds back a simulated system output to cancel the true system output so as to alleviate the effect of a pure time delay. More on the feedback structure with the Smith predictor will be discussed in the next paragraph. Note that D_i is a controller implemented in a femto BS and thus, d and h_i in Eq. (9) are estimated values in practice. The estimation error of d may result from network congestion dynamics and that of h_i may come from channel non-reciprocity in FDD, user mobility, etc. So, we let $d \to \hat{d}$ and $h_i \to \hat{h_i}$ in Eq. (9) to distinguish them from original ones. [9]

For better understanding of the resultant system, the system transfer function is rewritten by applying Eq. (8) to Eq. (6) as

$$I_F(z) = \frac{\sum_{i \in \mathcal{F}_u} D_i^*(z) z^{-d} a_i h_i (I_{th}(z) - I_M(z))}{1 + \sum_{i \in \mathcal{F}_u} D_i^*(z) a_i \hat{h_i} + \sum_{i \in \mathcal{F}_u} D_i^*(z) (z^{-d} a_i h_i - z^{-\hat{d}_i} a_i \hat{h_i})}. \tag{10}$$

Let's define W as the control input to D_i^*, then,

$$I_F(z) = \textstyle\sum_{i \in \mathcal{F}_u} W(z) D_i^*(z) z^{-d} a_i h_i. \tag{11}$$

Let $E_i(z) \triangleq W(z) D_i^*(z) (z^{-d} a_i h_i - z^{-\hat{d}} a_i \hat{h_i})$, then $E_i(z)$ can be interpreted as user i's output discrepancy resulting from the errors

[8] The z-transform of $x(k)$ s denoted by $x(z)$.

[9] In de facto cellular technologies, a user can measure channel gains to neighboring BSs and report the results to its serving BS. This report is called a *measurement report* in 3GPP specifications (e.g., UMTS and LTE). The measurement report can be triggered by a command from the serving BS, upon expiration of a timer at the user device, etc.

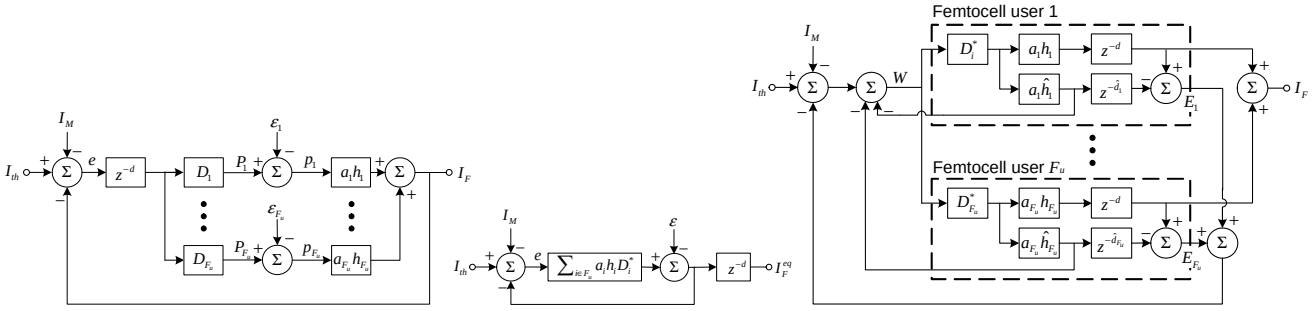

(a) MTXPC loop (b) Equivalent control loop (c) Redrawn MTXPC loop

Figure 5: MTXPC loop diagram

in estimating d and h_i. Then, equating Eqs. (10) and (11), and making a simplification, we get

$$W(z) = I_{th}(z) - I_M(z) - \sum_{i \in \mathcal{F}_u} (W(z) D_i^*(z) a_i \hat{h_i} + E_i(z)). \tag{12}$$

Based on Eqs. (11) and (12), we can redraw the system as in Fig. 5(c), in which each user has two feedback lines related to estimation errors with and without a delay component. This dual feedback structure provides a certain degree of robustness to the estimation errors of d and h_i. The simulation results in Section 6 show that the MTXPC loop has a bounded error against up to 100% overestimation of d and h_i.

5.1.2 Controller Design

In the equivalent system of Fig. 5(b), the controller output is not affected by the delay component. Thus, we can design D_i^* without considering the delay component. To avoid any drastic change of P_i, we use an additive increase/decrease to control it as

$$P_i(k+1) = P_i(k) + \Delta P_i(k) \tag{13}$$

and ΔP_i is controlled by a controller C_i based on e:

$$\Delta P_i(k) = C_i(e(k)). \tag{14}$$

Suppose that C_i is a linear controller. Then, P_i is expressed in the z-domain as

$$P_i(z) = D_i^*(z) e(z) = \frac{C_i(z)}{z-1} e(z). \tag{15}$$

Let $C_i = q_i C$ where q_i is a user-specific constant determined based on the user priority and control policy. C can be any type of controller. For simplicity of presentation, we define $Q \triangleq \sum_{i \in \mathcal{F}_u} a_i h_i q_i$.

5.1.3 Stability Analysis

As a special case, we consider a PI controller [15] for C as:

$$C(z) = K_P + K_I (1 - z^{-1})^{-1} \tag{16}$$

where K_P and K_I are constant.[10] For this C, we investigate stability and convergence to the optimal point under time-varying and unpredictable I_{th}, I_M and ε.

PROPOSITION 2. *With accurately estimated d and h_i, the MTXPC loop is stable if and only if*

$$0 < K_P < 2/Q, \;\; 0 < K_I < 4/Q - 2K_P.$$

PROOF. Without loss of generality, in a discrete-time system, an arbitrary time-varying signal X can be modeled as a piecewise constant model:

$$X(k) = \sum_{j=0}^{\infty} X_{0,j} \cdot 1(k - \tau_j) \tag{17}$$

where $1(k)$ is the unit step function, $X_{0,j} \in \mathbb{R}$, and τ_j a time lag. When $X(k)$ is input to a linear system, the output becomes a linear combination of the system outputs of $X_{0,j} \cdot 1(k - \tau_j)$ for $\forall j$. Therefore, the problem for an arbitrary input is reduced to that for a step input with an arbitrary amplitude. If d and h_i are estimated accurately, the control system becomes equivalent to that in Fig. 5(b), where $z^d I_F^{eq}(z) = Q\frac{C(z)}{z-1} e(z) - \varepsilon(z) = Q\frac{C(z)}{z-1}(I_{th}(z) - I_M(z) - z^d I_F^{eq}(z)) - \varepsilon(z)$. Thus, the system transfer function is

$$\begin{aligned} I(z) &= I_M(z) + z^d I_F^{eq}(z) \\ &= \frac{\frac{C(z)}{z-1}Q}{1 + \frac{C(z)}{z-1}Q} I_{th}(z) + \frac{1}{1 + \frac{C(z)}{z-1}Q}(I_M(z) - \varepsilon(z)) \end{aligned} \tag{18}$$

from which the system characteristic equation is obtained as

$$z^2 + (Q(K_P + K_I) - 2)z - QK_P + 1 = 0. \tag{19}$$

The system will be stable if and only if all roots of the characteristic equation are inside the unit circle. According to the Jury test [13], this condition is met for the characteristic equation $c(z) = z^2 + c_1 z + c_2$ when $1 - c_2^2 > 0$ and $1 - c_2^2 - \frac{(c_1 - c_1 c_2)^2}{1 - c_2^2} > 0$. From the first condition,

$$1 - c_2^2 = QK_P(2 - QK_P) > 0. \tag{20}$$

[10] The transient behavior of a PI controller is known to be generally more stable than a PID controller in the presence of noise. This is because the derivative action of a PID controller is sensitive to noise and causes jittery output. In the femtocell control system considered in this paper, there are several noise sources, such as other macrocells' interference, the gap between the maximum TX power and the actual one, etc. Thus, a PI controller is better suited for our problem.

If $QK_P > 0$, $0 < K_P < 2/Q$. If $QK_P < 0$, $K_P > 2/Q$ and no feasible K_P exists. From the second condition,

$$\frac{Q^2K_P^2(2-QK_P)^2 - Q^2K_P^2(Q(K_P+K_I)-2)^2}{QK_P(2-QK_P)} > 0 \tag{21}$$

which reduces to $(2-QK_P)^2 > (Q(K_P+K_I)-2)^2$ since $0 < K_P < 2/Q$, and hence $0 < K_I < 4/Q - 2K_P$. □

PROPOSITION 3. *The MTXPC loop converges to the optimal point, i.e., $e \to 0$, under unpredictable and time-varying I_{th}, I_M and ε.*

PROOF. The transfer function of $e(z)$ is obtained as

$$\begin{aligned} e(z) &= I_{th}(z) - I_M(z) - I_F(z) \\ &= I_{th}(z) - I_M(z) - \textstyle\sum_{i\in\mathcal{F}_u} a_i h_i D_i(z) z^{-d} e(z) - \varepsilon(z) \\ &= \left(1 - \frac{\sum_{i\in\mathcal{F}_u} a_i h_i D_i^*(z) z^{-d}}{1+\sum_{i\in\mathcal{F}_u} a_i h_i D_i^*(z)}\right)(I_{th}(z) - I_M(z) - \varepsilon(z)) \end{aligned} \tag{22}$$

where the second and the third equations follow from Eqs. (5) and (8), respectively. Provided the MTXPC loop is stable (by using the parameters within the range obtained in Proposition 2), according to the final value theorem [15], the final value of e in the time domain, denoted by e_∞, is obtained as $e_\infty = \lim_{z\to 1}(1-z^{-1})e(z)$. Since an arbitrary input of $I_{th}(z) - I_M(z) - \varepsilon(z)$ can be modeled as the sum of piecewise step functions, we only need to check convergence for a single step input, i.e., $\frac{zX_{0,j}}{z-1}$. Applying the final value theorem to Eq. (22),

$$\begin{aligned} e_\infty &= \lim_{z\to 1}(1-z^{-1})e(z) \\ &= \lim_{z\to 1}(1-z^{-1})\left(1 - \frac{\sum_{i\in\mathcal{F}_u} a_i h_i D_i^*(z) z^{-d}}{1+\sum_{i\in\mathcal{F}_u} a_i h_i D_i^*(z)}\right)\frac{zX_{0,j}}{z-1} \\ &= \lim_{z\to 1} X_{0,j}\left(1 - \frac{\sum_{i\in\mathcal{F}_u} a_i h_i C_i(z) z^{-d}}{z-1+\sum_{i\in\mathcal{F}_u} a_i h_i C_i(z)}\right) \\ &= 0 \end{aligned}$$

where the third equation follows from $D_i^*(z) = \frac{C_i(z)}{z-1}$. The above result is applicable to more general types of controller $C(z)$ than Eq. (16). □

Finally, in the original system of Fig. 5, using Eqs. (9), (15) and (16),

$$\begin{aligned} P_i(z) &= D_i(z) z^{-d} e(z) \\ &= \frac{q_i(\hat{Q}_K\hat{Q}^{-1} - K_P z^{-1})\cdot z^{-d} e(z)}{z + \hat{Q}_K - 2 - (K_P\hat{Q}-1)z^{-1} - \hat{Q}_K z^{-\hat{d}} + K_P\hat{Q}z^{-\hat{d}-1}} \end{aligned} \tag{23}$$

where $\hat{Q} = \sum_{i\in\mathcal{F}_u} a_i\hat{h}_i q_i$ and $\hat{Q}_K = (K_P+K_I)\hat{Q}$, and thus, P_i is obtained in the time domain as

$$\begin{aligned} P_i(k+1) = {} & [2-\hat{Q}_K]P_i(k) + (K_P\hat{Q}-1)P_i(k-1) \\ & + \hat{Q}_K P_i(k-\hat{d}) - K_P\hat{Q}P_i(k-\hat{d}-1) \\ & + q_i\hat{Q}_K\hat{Q}^{-1}e(k-d) - q_iK_P e(k-d-1). \end{aligned} \tag{24}$$

5.2 TSINRC Algorithm

The goal of the TSINRC algorithm is to allow femtocell users to reach a *Nash equilibrium* [16] in a fully-distributed manner by solving $P2$. We first define the utility function of femtocell users and then show that the solution of $P2$ is a Nash equilibrium. Finally, we develop an instantly convergent algorithm to achieve the target SINR.

Let us define the utility function of femtocell user i as

$$u_i(p_i, \gamma_i) = g(\gamma_i, a_i) - \mu_i a_i h_i p_i \tag{25}$$

which follows the general form proposed by Ji and Huang [9]. In the femtocell problem, the first and second terms of RHS in Eq. (25) can be interpreted as a reward for utility gain and a penalty for interference to macrocells, respectively, as pointed out by Vikram *et al.* [4]. Here, p_i and γ_i have the following relationship:

$$\gamma_i = \frac{h_{i,S(i)}p_i}{I_M^i + I_F^i + \sigma^2} \triangleq \frac{h_{i,S(i)}p_i}{I_i(\mathbf{p}_{-i})} \tag{26}$$

where $S(i)$ is user i's serving femto BS; I_M^i and I_F^i are the UL interference levels to femtocell user i due to macrocell users and other femtocell users, respectively; $\mathbf{p}_{-i}$ is the TX power vector of all but femtocell user i, and $I_i(\mathbf{p}_{-i})$ indicates the UL interference plus the thermal noise user i experiences.

For g, we consider the following family of utility functions parameterized by $\alpha \geq 0$ [17]:

$$g(\gamma, a) = \begin{cases} (1-\alpha)^{-1}x(\gamma,a)^{1-\alpha} & \alpha \neq 1 \\ \log x(\gamma, a) & \alpha = 1 \end{cases} \tag{27}$$

where $x(\gamma, a)$ is the throughput achieved by SINR γ and activity factor a. In particular, if $\alpha = 0$, g reduces to throughput. If $\alpha = 1$, proportional fairness among competing users is attained; if $\alpha = 2$, then harmonic mean fairness; and if $\alpha \to \infty$, then max-min fairness [18]. We consider the Shannon's channel capacity function for x, i.e., $x(\gamma, a) = aB\log_2(1+\gamma)$, with channel bandwidth B [19]. We simply denote $x_i = x(\gamma_i, a_i)$ and $g(x_i) = g(\gamma_i, a_i)$.

PROPOSITION 4. *A Nash equilibrium exists in the non-cooperative game of $P2$.*

PROOF. From [20], a Nash equilibrium exists in $P2$ if

C1. the feasible region of $\mathbf{p}$ is a nonempty, convex, and compact subset of some Euclidean space $\mathbb{R}^{F_u}$; and

C2. u_i is continuous in $\mathbf{p}$ and quasi-concave in p_i for $\forall i \in \mathcal{F}_u$.

We show that $P2$ meets the above two conditions as follows.

The feasible region of $\mathbf{p}$ is $\{\mathbf{p} | 0 \preceq \mathbf{p} \preceq \mathbf{P}\}$, thus meeting the first condition. It is straightforward to show that $\partial u_i/\partial\gamma_i \geq 0$ and $\partial^2 u_i/\partial\gamma_i^2 \leq 0$, which confirms that, given fixed p_i, u_i is a monotonically increasing concave upward function of γ_i. Likewise, given fixed γ_i, u_i is a monotonically decreasing concave downward function of p_i since $\partial u_i/\partial p_i \leq 0$ and $\partial^2 u_i/\partial p_i^2 \geq 0$. Therefore, u_i is quasi-concave in p_i. It is also clear that u_i is continuous in $\mathbf{p}$. □

Based on the result in [9], if a Nash equilibrium exists in $P2$, the equilibrium should satisfy $\partial u_i/\partial p_i = 0$. $\partial u_i/\partial p_i$ is obtained from Eqs. (25), (26), and (27) as

$$\begin{aligned} \frac{\partial u_i}{\partial p_i} &= \frac{\mathrm{d}g}{\mathrm{d}x_i}\frac{\mathrm{d}x_i}{\mathrm{d}\gamma_i}\frac{\mathrm{d}\gamma_i}{\mathrm{d}p_i} - \mu_i a_i h_i \\ &= \frac{\mathrm{d}g}{\mathrm{d}x_i}\frac{a_i B}{(\log 2)(1+\gamma_i)}\frac{h_{i,S(i)}}{I_i(\mathbf{p}_{-i})} - \mu_i a_i h_i. \end{aligned} \tag{28}$$

Let us define a function H as

$$H(\gamma_i) \triangleq \frac{g'(x_i)}{(\log 2)(1+\gamma_i)}. \tag{29}$$

Then, $\partial u_i/\partial p_i = 0$ in $[0, P_i]$ yields

$$\gamma_i^* = \min\left\{\left[H^{-1}\left(\tfrac{\mu_i h_i I_i(\mathbf{p}_{-i})}{B h_{i,S(i)}}\right)\right]^+, \tfrac{h_{i,S(i)}P_i}{I_i(\mathbf{p}_{-i})}\right\}. \tag{30}$$

Based on this result, we design the TSINRC algorithm as

$$\gamma_i^{(l+1)} = \min\left\{\left[H^{-1}\left(\frac{\mu_i h_i I_i(\mathbf{p}_{-i}^{(l)})}{B h_{i,S(i)}}\right)\right]^+, \frac{h_{i,S(i)}P_i}{I_i(\mathbf{p}_{-i}^{(l)})}\right\} \quad (31)$$

where $I_i(\mathbf{p}_{-i}^{(l)})$ indicates the interference observed in iteration interval l. For example, if $\alpha = 0$ for throughput maximization, $H(\gamma) = \frac{1}{(\log 2)(1+\gamma)}$ and $H^{-1}(y) = \frac{1}{(\log 2)y} - 1$. If $\alpha = 1$ for proportional fairness, $H(\gamma) = [a_i B(1+\gamma_i)\log(1+\gamma_i)]^{-1}$ and $H^{-1}(y) = L[a_i B y \mathcal{W}(\frac{L}{a_i B y})]^{-1} - 1$ where $\mathcal{W}$ denotes the Lambert's *W* function and $L = \ln(10)$.

The sufficient condition for the TSINRC algorithm to converge to γ_i^* in Eq. (30) is stated as follows.

PROPOSITION 5. *$\mu_i = \lambda_i I_i^{-1}(\mathbf{p}_{-i})$ is a sufficient condition for convergence of the TSINRC algorithm.*

If $\mu_i = \lambda_i I_i^{-1}(\mathbf{p}_{-i})$, $H^{-1}(\frac{\mu_i h_i I_i(\mathbf{p}_{-i}^{(l)})}{B h_{i,S(i)}}) = H^{-1}(\frac{\lambda_i h_i}{B h_{i,S(i)}})$ becomes a constant. Therefore, the TSINRC algorithm immediately converges to γ_i^*. Intuitively, $\mu_i = \lambda_i I_i^{-1}(\mathbf{p}_{-i})$ means giving a less penalty to users who are suffering higher UL interference. Due to the nature of immediate convergence under this setting, the TSINRC algorithm can operate asynchronously with the MTXPC algorithm.

5.3 ITXPC Algorithm

The TSINRC algorithm tracks the target SINR by controlling the instantaneous TX power of a femtocell user. The control system is simply expressed as Eq. (26), which has a nonlinear relationship between components. For analytical tractability, we need to linearize the relationship. We first take the log of both sides of Eq. (26) and a log change of variables: $\widetilde{h}_{i,S(i)} = \log h_{i,S(i)}$, $\widetilde{p}_i = \log p_i$, $\widetilde{I}_i(\mathbf{p}_{-i}) = \log I_i(\mathbf{p}_{-i})$, and consequently, $\widetilde{\gamma}_i = \log \gamma_i = \widetilde{h}_{i,S(i)} + \widetilde{p}_i - \widetilde{I}_i(\mathbf{p}_{-i})$. Then, we replace the original error function $e_i = \gamma_i^* - \gamma_i$ defined in $P3$ with $\widetilde{e}_i = \widetilde{\gamma_i^*} - \widetilde{\gamma}_i$. Clearly, $\widetilde{e}_i \to 0$ if and only if $e_i \to 0$, making the modified problem valid.

Due to the bursty nature of the UL interference to femtocells, the controller should guarantee that the TX power converges without overshoot or oscillation. We adopt an additive increase/decrease control for $\widetilde{p}_i$:

$$\widetilde{p}_i(t+1) = \widetilde{p}_i(t) + K_i \widetilde{e}_i(t) \quad (32)$$

where K_i is constant. Then, the system transfer function is

$$E(z) = \frac{z-1}{z+K_i-1}(\widetilde{\gamma_i^*}(z) + \widetilde{I}_i(\mathbf{p}_{-i})(z) - \widetilde{h}_{i,S(i)}(z)) \quad (33)$$

and, by applying the inverse z-transform, the time domain response to an arbitrary step input is simply obtained as

$$\widetilde{e}_i(t) = X_0(1-K_i)^t \quad (34)$$

where X_0 is the step input amplitude. Therefore, if $0 < K_i \leq 1$, $\widetilde{e}_i$ converges without overshoot and oscillation, and so does e_i. It also implies that the ITXPC algorithm converges against time-varying target SINR, UL interference, and channel gain (even with measurement error). Finally, the time-domain expression of the algorithm is given as

$$p_i(t+1) = 10^{\widetilde{p}_i(t+1)} = p(t) \cdot 10^{K_i \widetilde{e}_i(t)}. \quad (35)$$

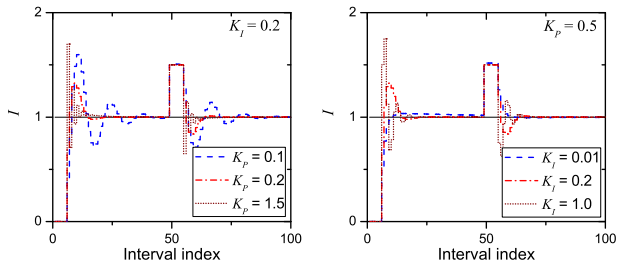

Figure 6: Step response of the MTXPC loop

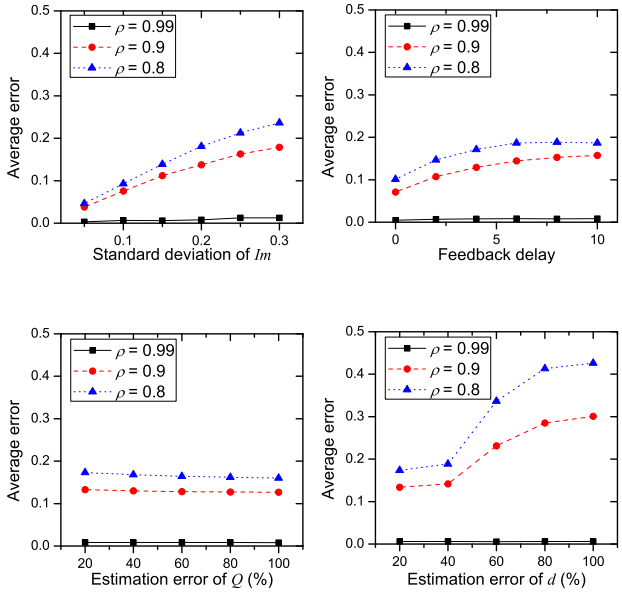

Figure 7: Performance of the MTXPC loop under correlated Gaussian I_M (Q = 1, d = 5)

6. EVALUATION

To evaluate the effectiveness of CTRL, we first investigate the performance of each control loop in controllable environments. We then simulate multi-cell networks in more realistic environments.

6.1 Evaluation of Control Algorithms

The MTXPC algorithm has two configuration parameters, K_P and K_I, which dictate its convergence behavior. Fig. 6 shows the response of the MTXPC loop to the step inputs $I_{th}(0) = 1$ and $I_M(50) = 1$ when $Q = 1$ and $d = 5$. The MTXPC loop is shown to converge only after going through a short transient state, with K_P and K_I values in the range specified in Proposition 2. As K_P increases, MTXPC becomes more responsive, but exhibits overshoot and oscillation with too high K_P. A similar trend is observed in K_I while the convergence becomes slow if K_I is too small (= 0.01).

The error performance $E[|e|]$ (averaged over time) of the MTXPC loop against a time-varying macrocell load is plotted in Fig. 7. The macrocell load is modeled as a correlated Gaussian random variable with autocorrelation ρ. The figure shows the trend that the error increases as the load changes faster (higher ρ), the load has a

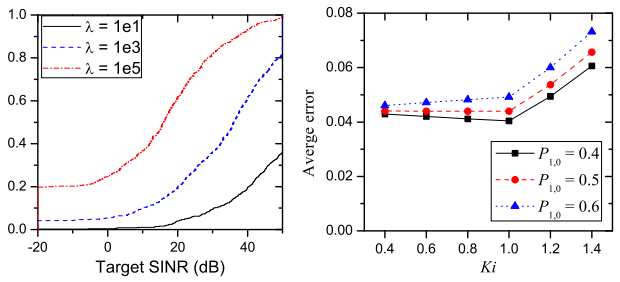

Figure 8: Cumulative distribution of a femtocell user's target SINR ($\alpha = 0$) and the error performance of the ITXPC loop against bursty interference

larger deviation and the feedback delay gets longer. It is also shown that the MTXPC loop is stable (i.e., bounded error) against up to 100% overestimation of Q and d. Surprisingly, a higher estimation error of Q leads to a slightly better error performance. This is because a larger $\hat{Q}$ enhances the loop's responsiveness. However, when $\hat{Q}$ increases beyond a certain point, the loop becomes unstable and diverges.

The left figure of Fig. 8 shows the cumulative distribution function (cdf) of the target SINR determined by the TSINRC loop when femtocells (each with a single user) are uniformly distributed within a circular macrocell and $\alpha = 0$. The cdf is shown to depend strongly on λ. Therefore, an inappropriate λ value can cause femtocell users to have too high target SINRs, generating high interference to macrocells. This configuration problem of the TSINRC loop is complemented by the MTXPC loop. The right figure shows the time-averaged error performance $E[|e_i|]$ of the ITXPC loop while K_i is varied. The UL interference is modeled as a two-state Markov chain where interference exists only in an active state. The idle-to-active transition probability $P_{0,1}$ is fixed at 0.5. Then, the active-to-idle transition probability $P_{1,0}$ determines the burstiness of interference. $K_i = 1$ means immediate adjustment of TX power to meet the target SINR in the next slot, and thus achieves the highest performance against less bursty interference ($P_{1,0} = 0.4$), but lower performance against more bursty interference ($P_{1,0} = 0.6$). When $K_i > 1$, the average error increases due to overshoot and oscillation.

6.2 Simulation of Multi-Cell Networks

As a realistic communication environment, we consider a two-tier hexagonal cellular network comprised of 7 macrocells, each with a single sector. The inter-site distance (ISD) is $500\sqrt{3} \approx 866$ meters. Macrocell users and femto BSs are randomly distributed within 500 meters to the closest macro BS; the angle and the distance of each to the macro BS are randomly chosen with a uniform probability distribution. Unless specified otherwise, within each macrocell, the number of macrocell users (M_u/M) and that of femtocells (F/M) are set to 50 and 100, respectively. Each femto BS serves a single user that is also randomly distributed within 50 meters from it. The channel gains of a user to BSs are determined based on the ITU and COST231 models which are described as [21][22]:

- macrocell user to marco BS (outdoor link):

$$h = 10^{4.9} \left(\frac{r}{1000}\right)^4 f^3 10^{S/10};$$

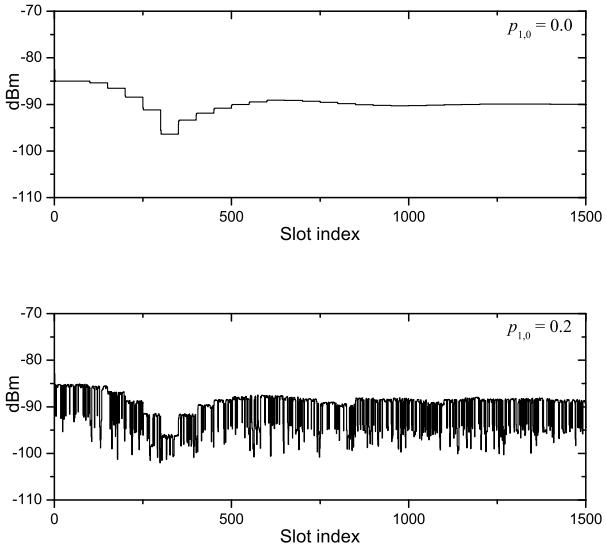

Figure 9: Time evolution of I under static (top) and dynamic (bottom) user traffic patterns

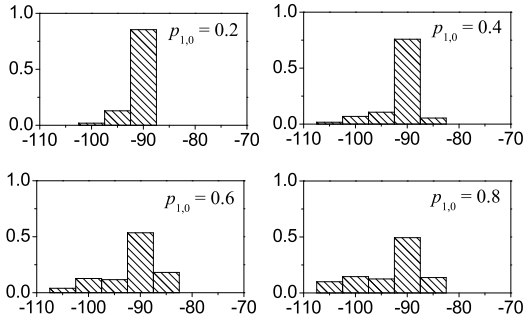

Figure 10: Probability distribution of I over time under various user-activity patterns

- macrocell user to femto BS, femtocell user to macro BS (outdoor-to-indoor or indoor-to-outdoor link):

$$h = 10^{4.9} \left(\frac{r}{1000}\right)^4 f^3 10^{S/10} 10^{(L_i+L_e)/10};$$

- femtocell user to femto BS (indoor link):

$$h = 10^3 r^{3.7} 10^{S/10} 10^{L_i/10},$$

where r is the transmitter-receiver separation distance in meters; f the carrier frequency in MHz; S the log-normal shadowing factor with a standard deviation of 8 dB; L_i and L_e are internal and external wall losses and set to 2 and 7 dB, respectively, in our simulation.

Both macro and femto BSs operate at the carrier frequency of 2.5 GHz with 5 MHz channel bandwidth. We use slot as the time unit, and assume that user TX activities (ON/OFF) and instantaneous TX power change within a slot.[11] To determine a macrocell user's TX power, we use an immediate adjustment approach corresponding to $K_i = 1$ in the ITXPC loop as explained in the previous subsection.

[11] A slot corresponds to the duration of transmitting a frame, which is 10 or 20 ms in UMTS.

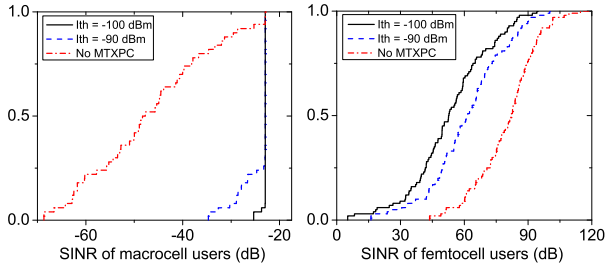

Figure 11: Cumulative distribution of achieved SINR with and without MTXPC under different load thresholds

The target E_b/N_0 of macrocell users is set to 7 dB with the bit rate of 8 kbps. This corresponds to a toll-quality voice call with the bit error rate less than 10^{-3} [23] and the SINR of -20.96 dB. A user's activity in a slot is determined again by a two-state (active/idle) Markov chain. We fix the idle-to-active transition probability at 0.5. The minimum and maximum TX power inherently given to user devices are assumed to be -50 and 20 dBm, respectively. The feedback interval T of the MTXPC loop is set to 50 slots. The macrocell feedback delay is $5T$ ($d = 5$). We set q_i to 1 for $\forall i \in \mathcal{F}_u$, $K_P Q$ and $K_I Q$ to 0.5 and 0.2, respectively, and K_i to 0.8.

Fig. 9 shows the time evolution of I for $I_{th} = -90$ dBm at the center macrocell when $P_{1,0} = 0$ (top) and $P_{1,0} = 0.2$ (bottom). 30 macrocell users and 50 femto BSs are distributed in each macrocell. In both cases, CTRL converges to I_{th} and thus successfully protects the macrocell's UL communication. Since T = 50 slots, the MTXPC loop converges within less than 20 feedback intervals. Under a dynamic user traffic pattern (bottom), I fluctuates somewhat, but the average is still close to I_{th} (that of the last 500 samples is -90.03 dBm). The robustness of CTRL against dynamic user activities is investigated further in Fig. 10. Although CTRL achieves I_{th} in most of the observed slots, the variance increases as $P_{1,0}$ gets higher, which is somewhat inevitable due to the delayed feedback.

In Fig. 11, we compare the cdfs of the achieved SINRs by macrocell users (left) and femtocell users (right), with and without the MTXPC loop and for different load thresholds. For resource utilization within femtocells without MTXPC, we assume that only TSINRC and ITXPC loops are used. $P_{1,0}$ is set to 0.2. Two cases of I_{th} are considered (-100 and -90 dBm). The left figure shows that, with MTXPC, 96% (I_{th} = -100 dBm) and 74% (I_{th} = -90 dBm) of the macrocell users successfully achieve their target SINR (-20.96 dB) while, without MTXPC, only 8% of macrocell users achieve the target. These users are those close to their serving BSs and thus have enough room to increase their TX power against excessive UL interference. As shown in the right figure, femtocell users without MTXPC achieve better performance than with MTXPC at the expense of macrocell users' performance degradation. On the other hand, it is observed that a lower load threshold improves the performance of macrocell users while degrading that of femtocell users. That is, the load threshold controls the tradeoff between macrocell and femtocell capacities.

Next, we study the effect of the number of macrocell and femtocell users. The corresponding simulation results are plotted in Fig. 12 where I_{th} is set to -100 dBm. The left top figure shows that CTRL successfully protects the macrocell's UL service regardless of the number of femtocell users. However, without MTXPC, if the number of femtocell users (F/M) is increased from 50 to 100,

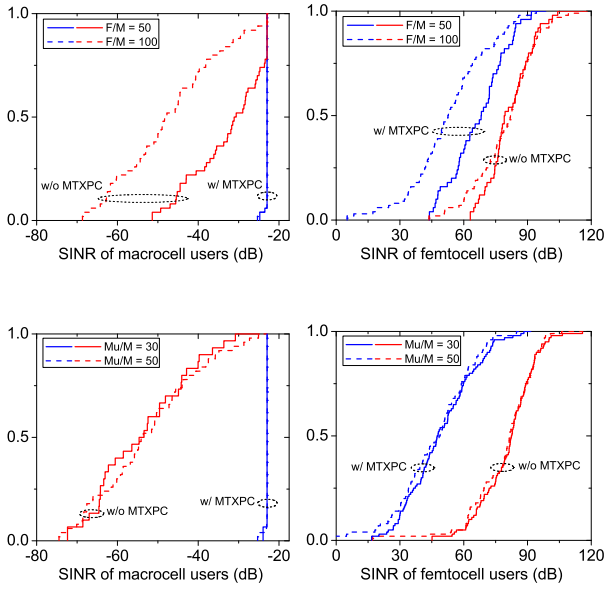

Figure 12: Cumulative distribution of achieved SINR under different numbers of macrocell and femtocell users

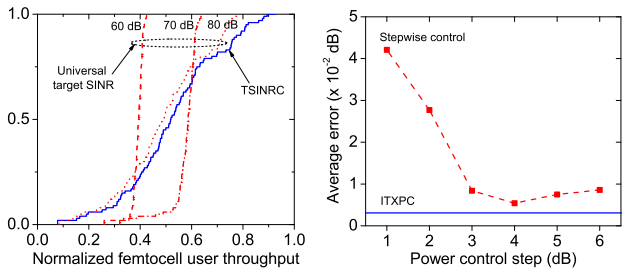

Figure 13: Cumulative distribution of femtocell users' throughput with the universal target SINR and with TSINRC (left), and the average control error with the stepwise power control and with ITXPC (right)

most macrocell users' services get deteriorated significantly. As shown in the right top figure, increasing the number of femtocell users degrades their performance as well due to the increased inter-femtocell interference. Such performance degradation of femtocell users is somewhat limited when MTXPC is used. This is because the total amount of the radiated interference from femtocell users to macro BSs is controlled by MTXPC and thus, that between femtocell users also gets limited to some degree. In the bottom figures, the number of macrocell users (M_u/M) is shown to not affect the performance much. With MTXPC, the increased number of macrocell users slightly degrades the performance of femtocell users due to the reduced load portion allowed for femtocell users. Another observation from the right bottom figure is that the worst group of femtocell users get deteriorated considerably as the number of macrocell users increases. This trend results from the increased possibility of the presence of nearby macrocell users producing bursty UL interference to femtocells.

Finally, Fig. 13 shows the effectiveness of TSINRC (left) and

ITXPC (right) by replacing them with simpler schemes. First, the left figure compares TSINRC with the case when all femtocell users employ an identical target SINR (referred to as the *universal target SINR* case). When the universal target SINR is configured to 60 dB, a significant capacity loss occurs, compared to TSINRC, although some femtocell users with poor channel quality experience better performance thanks to the reduced interference. When it is as high as 80 dB, most users experience worse performance than those with TSINRC and none of them even achieves the target due to the excessive interference. On the other hand, the universal target SINR of 70 dB seems to achieve balanced performance distribution among femtocell users with a moderate capacity loss. However, finding an appropriate universal target SINR is not easy in practice. It may require the global status information of the network, such as all users' channel gains and activity factors. Second, in the right figure, ITXPC is compared to the stepwise power-control scheme which is widely used in conventional cellular systems. As shown in the figure, the average control error of the stepwise control ($E[|\widetilde{e_i}|]$) is a convex function of the step size, and thus, there exists a unique, best step size. However, the best step size may differ for different users due to different interference patterns. ITXPC is shown to achieve better performance than the stepwise control even with the best step size.

7. CONCLUSION

In this paper, we have presented a novel femtocell-management framework, CTRL, for cellular networks. CTRL is composed of three complementary control loops—MTXPC, TSINRC, and ITXPC—that protect the macrocell's uplink communication, coordinate resource usage among femtocells, and protect the femtocells' uplink communications. Based on the complementary interactions between the control loops, CTRL enables spatial reuse of channel resources within femtocells without degrading macrocell users' performance regardless of the number of femtocells in a macrocell. CTRL is easily deployable in existing cellular networks without any change of the RRM of macro BSs. Moreover, CTRL ensures distributed and self-organizing operation thanks to its convergence even in the presence of time-varying and unpredictable environmental changes.

Acknowledgement

The work reported in this paper was supported in part by the NSF under Grant CNS-0721529.

8. REFERENCES

[1] *3G Home NodeB Study Item*, 3GPP Technical Report 25.820, Rev. 8.2.0, Sept. 2008.

[2] V. Chandrasekhar, J. Andrews, and A. Gatherer, "Femtocell networks: a survey," *IEEE Communications Magazine*, vol. 46, no. 9, pp. 59 –67, Sept. 2008.

[3] M. Yavuz, F. Meshkati, S. Nanda, A. Pokhariyal, N. Johnson, B. Raghothaman, and A. Richardson, "Interference management and performance analysis of UMTS/HSPA+ femtocells," *IEEE Communications Magazine*, vol. 47, no. 9, pp. 102 –109, Sept. 2009.

[4] V. Chandrasekhar, J. Andrews, T. Muharemovic, Z. Shen, and A. Gatherer, "Power control in two-tier femtocell networks," *IEEE Transactions on Wireless Communications*, vol. 8, no. 8, pp. 4316 –4328, Aug. 2009.

[5] V. Chandrasekhar and J. Andrews, "Uplink capacity and interference avoidance for two-tier femtocell networks," *IEEE Transactions on Wireless Communications*, vol. 8, no. 7, pp. 3498 –3509, July 2009.

[6] H.-S. Jo, C. Mun, J. Moon, and J.-G. Yook, "Interference mitigation using uplink power control for two-tier femtocell networks," *IEEE Transactions on Wireless Communications*, vol. 8, no. 10, pp. 4906 –4910, Oct. 2009.

[7] L. Ho and H. Claussen, "Effects of user-deployed, co-channel femtocells on the call drop probability in a residential scenario," Sept. 2007, pp. 1 –5.

[8] K. Sundaresan and S. Rangarajan, "Efficient resource management in OFDMA femto cells," in *MobiHoc '09: Proceedings of the tenth ACM international symposium on Mobile ad hoc networking and computing*. New York, NY, USA: ACM, 2009, pp. 33–42.

[9] H. Ji and C.-Y. Huang, "Non-cooperative uplink power control in cellular radio systems," *Wireless Networks*, vol. 4, no. 3, pp. 233–240, Mar. 1998.

[10] H. Wicaksana, S. Ting, C. Ho, W. Chin, and Y. Guan, "AF two-path half duplex relaying with inter-relay self interference cancellation: diversity analysis and its improvement," *IEEE Transactions on Wireless Communications*, vol. 8, no. 9, pp. 4720 –4729, Sept. 2009.

[11] *Radio Resource Control (RRC) Protocol Specification (Release 8)*, 3GPP Technical Specification 25.331, Rev. 8.4.0, Sept. 2008.

[12] A. J. Viterbi, *CDMA: Principles of Spread Spectrum Communication*. Addison-Wesley, 1995.

[13] K. J. Astrom and B. Wittenmark, *Computer-Controlled Systems: Theory and Design*. Prentice Hall, 1996.

[14] J. E. Normey-Rico and E. F. Camacho, *Control of Dead-time Processes*. Springer, 2007.

[15] G. F. Franklin, J. D. Powell, and A. Emami-Naeini, *Feedback Control of Dynamic Systems*. Prentice Hall, 1994.

[16] J. Nash, "Non-cooperative games," *The Annals of Mathematics*, vol. 54, no. 2, pp. 286–295, 1951. [Online]. Available: http://www.jstor.org/stable/1969529

[17] J. Mo and J. Walrand, "Fair end-to-end window-based congestion control," *IEEE/ACM Transactions on Networking*, vol. 8, no. 5, pp. 556 –567, Oct. 2000.

[18] J.-W. Lee, M. Chiang, and A. Calderbank, "Utility-optimal random-access control," *IEEE Transactions on Wireless Communications*, vol. 6, no. 7, pp. 2741 –2751, July 2007.

[19] B. Sklar, *Digital Communications: Fundamentals and Applications*. Prentice Hall PTR, 2001.

[20] J. F. Nash, "Equilibrium points in n-person games," in *Proc. Natl. Acad. Sci. U.S.A.*, vol. 36, no. 1, Jan. 1950, pp. 48–49.

[21] *Guidelines for evaluation of radio transmission technologies for IMT-2000*, ITU-R Rec M.1225, Feb. 1997.

[22] "Digital mobile radio towards future generation systems," European Communities, COST Action 231 EUR 18957, 1999.

[23] K. Gilhousen, I. Jacobs, R. Padovani, A. Viterbi, J. Weaver, L.A., and I. Wheatley, C.E., "On the capacity of a cellular CDMA system," *IEEE Transactions on Vehicular Technology*, vol. 40, no. 2, pp. 303 –312, May 1991.